Published in final edited form as:
Am J Hematol. 2009 February ; 84(2): 65–70. doi:10.1002/ajh.21319.

Generation and phenotyping of *mCd59a* and *mCd59b* double-knockout mice

Xuebin Qin[1,2,*], **Weiguo Hu**[2], **Wenping Song**[2], **Luciano Grubissich**[2], **Xuemei Hu**[2], **Gongxiong Wu**[2], **Sean Ferris**[2], **Martin Dobarro**[2], and **Jose A. Halperin**[1,2]

[1]Department of Medicine, Brigham and Women's Hospital, Boston, Massachusetts

[2]Harvard Medical School, Laboratory for Translational Research, Cambridge, Massachusetts

Abstract

CD59 is a membrane protein inhibitor of the membrane attack complex (MAC) of complement. Humans express only one, whereas mice express two *CD59* genes. We previously reported the targeted deletion of the *mCd59b* gene in which absence of mCd59b together with an unintended down regulation of mCd59a caused hemolytic anemia with spontaneous platelet activation. To confirm the complement role in the hemolytic anemia caused by abrogation of mCd59 function, we have developed a *mCd59a* and *mCd59b* double knock out mice and analyzed its phenotype in complement sufficient and deficient ($C3^{-/-}$). We report here that total abrogation of mCd59 function in $mCd59ab^{-/-}$ mice results in complement-mediated hemolytic anemia that is rescued by the deficiency of C3 in compound $mCd59ab^{-/-}/C3^{-/-}$ mice.

Introduction

The complement system is an effector of the immune system that mediates both acquired and innate responses [1]. The system consists of more than 30 soluble plasma proteins that interact in three distinct enzymatic activation cascades known as the classical, alternative, and lectin pathways [1,2]. The three activation pathways eventually converge at the level of C3 to form a C5-convertase that activates the common terminal cascade leading to polymerization of C9 and formation of the membrane attack complex (MAC) [1,2]. The MAC is a macromolecular pore that inserts into the cell membrane causing influx of ions and water, eventually leading to colloid-osmotic swelling and lysis of the target cell (lytic MAC). In contrast, transient opening of MAC (nonlytic MAC) pores can generate significant changes in membrane permeability and internal composition of the target cell without compromising its viability [3–6].

The potentially harmful effect of autologous complement activation on self cells is attenuated by more than 10 plasma- and membrane-bound inhibitory proteins that restrict complement activation at different stages of the activation pathways [5,7]. The delicate

[*]Correspondence to: Dr. Xuebin Qin, Harvard Medical School, One Kendall Square, Building 600, 3rd Floor, Cambridge, MA 02139. xuebin_qin@hms.harvard.edu.

Conflict of Interest: Nothing to report.

balance between complement activation and restriction on autologous cells is subject to perturbation by either increased complement activation or decreased attenuation. For example, in auto-immune diseases such as systemic lupus erythematosus or glomerulonephritis, severe organ damage results from immune-complex activation of the classical complement pathway [5,8]. Conversely, a deficiency of glycan phosphatidylinositol (GPI)-linked complement-regulatory proteins such as DAF and CD59 in circulating cells—due to an acquired somatic mutation of the PIG-A gene—is responsible for the hemolytic anemia that characterizes paroxysmal nocturnal hemoglobinuria (PNH) [9–12]. PNH-hemolytic anemia is mediated by MAC-induced lysis of erythrocytes lacking CD59 and DAF [9,12].

Several lines of evidence from human and animal studies indicate that CD59 is more relevant than DAF in protecting red blood cells from MAC formation and MAC-induced phenomena [5]. Interestingly, humans have only one *CD59* gene, whereas mice have two *Cd59* genes (termed *mCd59a* and *mCd59b*) [13,14]. Single *mCd59a* and *mCd59b* knockout mice showing intravascular hemolysis have been reported [15,16]. The *mCd59b* knock out mouse reported by our group had a stronger PNH-like phenotype because of the absence of mCd59b function combined with an unintended significant down-regulation of mCd59a [17].

The fact that each *mCd59* gene has two promoters that control the expression of different *mCd59* transcripts in a tissue-specific manner [17] suggests differential and potentially complex regulation in different tissues. On the basis of this consideration, we engaged in an effort to develop a *mCd59a* and *mCd59b* double-knockout mouse ($mCd59ab^{-/-}$) that we plan to use in studies on the role of complement in human diseases. Here, we report the targeted deletion of both *mCd59* genes and the use of these mice in complement-sufficient ($mCd59ab^{-/-}/C3^{+/+}$) and complement-deficient ($mCd59ab^{-/-}/C3^{-/-}$) backgrounds to confirm the role of complement in the hemolytic phenotype observed in CD59 deficient mice.

Results

Generation of mCd59a and mCd59b double-knockout mice

To generate a *mCd59a* and *mCd59b* double knockout mouse, we undertook a targeted deletion strategy (Fig. 1a), because the very short genetic (~0.005 cM) and physical (~10 kb) distance between the genes practically precluded a recombination-dependent ($mCd59a^{-/-}$ and $mCd59b^{-/-}$) approach [14]. The target vector was specifically designed to remove simultaneously a 24 kb genomic fragment encompassing (1) exon 4 of *mCd59b*, which encodes ~60% of the functional peptide including its active site [18,19] plus a 20-amino-acid putative GPI anchor attachment peptide [13], and (2) exons 1 and 2 of *mCd59a*, which encode for its start codon and N-terminal signal peptide [13,14]. A database search using the 11.6-kb genomic fragment located between the *mCd59b* and *mCd59a* genes indicated that this region, which would be also deleted by our construct, did not contain either known genes or expressed sequence tags (EST). Southern blotting confirmed that homologous recombination for both arms of the targeting cassette occurred in two independent 129 ES cell lines that were selected for microinjection into B6 blastocytes (Fig. 1b). Resulting

chimeras crossed with B6 mice yielded *mCd59ab*$^{+/-}$ on a 129/B6 mixed genetic background. Intercrossing *mCd59ab*$^{+/-}$ mice generated *mCd59ab*$^{-/-}$, *mCd59ab*$^{+/-}$, and *mCd59ab*$^{+/+}$ offspring in the expected Mendelian ratio. The genotype of the offspring was determined by PCR using the specific primers shown in Fig. 1c. The successful disruption of both *mCd59a* and *mCd59* genes was confirmed by (1) Northern analysis with *mCd59a*- and *mCd59b*-specific probes (Fig. 1d,e) showing absence of both *mCd59a* and *mCd59b* mRNA transcripts in multiple tissues, and (2) FACS analysis with specific anti-mCd59a and mCd59b monoclonal antibodies showing the physical absence of both mCd59 proteins in erythrocytes (data not shown) as reported in Ref. 17 and in platelets of several *mCd59ab*$^{-/-}$ mice (Fig. 2a and 2b, and Table I). All the experimental mice referred to below were in pure B6 genetic background. The life-span of *mCd59ab*$^{-/-}$ is about 2 years, similar to that of *mCd59ab*$^{+/+}$ mice. Parturation of *mCd59ab*$^{-/-}$ was not affected and similar to that of *mCd59ab*$^{+/+}$.

Erythrocytes from *mCd59ab*$^{-/-}$ mice are more sensitive to complement-mediated lysis

CD59 protects erythrocytes from complement-mediated lysis. The complete functional deficiency of mCd59 in *mCd59ab*$^{-/-}$ mice was confirmed by the increased sensitivity of *mCd59ab*$^{-/-}$ erythrocytes to complement-mediated lysis when compared with *mCd59ab*$^{+/+}$, *mCd59ab*$^{+/-}$, and *mCd59b*$^{-/-}$ (the latter shown to exhibit absence of mCd59b and down-regulation of mCd59a).

To assess the complement sensitivity of *mCd59ab*$^{-/-}$ erythrocytes *ex vivo*, we used different methods of complement activation as described in Ref. 16: (a) Ham's assay, the clinical test for diagnosis of PNH in humans, in which complement is activated by serum acidification (Fig. 3a); (b) Cobra venom factor (CVF) assay, in which CVF is used to activate the alternative complement pathway (Fig. 3b); (c) classical pathway assay in which complement is activated by antigen-antibody complexes (Fig. 3c); and (d) the MAC assay that uses C8-deficient serum to form C5b-7 complexes on erythrocyte membranes plus mouse serum supplemented with 10 mM EDTA as a source of mouse C8 and C9 (Fig. 3d). In all these assays, *mCd59ab*$^{-/-}$ erythrocytes exhibited significantly higher sensitivity to complement-mediated lysis when compared with either *mCd59ab*$^{+/+}$ or *mCd59ab*$^{+/-}$ erythrocytes (see Fig. 3). Furthermore, *mCd59ab*$^{-/-}$ erythrocytes were significantly more sensitive to complement-mediated lysis than *mCd59b*$^{-/-}$ erythrocytes, illustrating the functional significance of both *mCd59* genes (Fig. 3e). This increased sensitivity of *mCd59ab*$^{-/-}$ erythrocytes to complement- mediated lysis is not associated with a concomitant down-regulation of other complement regulatory membrane proteins as documented by FACS analysis with anti-mDAF and anti-mCrry specific antibodies (Fig. 3f).

Complement-mediated hemolytic anemia in *mCd59ab*$^{-/-}$ mice

Consistent with the previous findings, *mCd59ab*$^{-/-}$ mice showed complement-mediated hemolytic anemia characterized by a significantly lower blood hemoglobin concentration and a significantly increased reticulocyte count when compared with *mCd59ab*$^{+/-}$ or *mCd59ab*$^{+/+}$ *mice* (Table II, and Fig 4a–e). In the pure B6 genetic background of the mice used for this study, 35% of the *mCd59ab*$^{-/-}$ mice exhibited hemoglobin values lower than 13 gr/dl, which is 2SD below the mean value of wild type B6 mice. Hemolytic anemia in

mCd59ab$^{-/-}$ mice was complement-mediated because it was rescued by C3 deficiency, as shown in *mCd59ab*$^{-/-}$/*C3*$^{-/-}$ mice in which hematological parameters are similar to those in *mCd59ab*$^{+/+}$/*C3*$^{+/+}$ mice.

Progressive loss of male fertility in *mCd59ab*$^{-/-}$ mice

We have reported that *mCd59b*$^{-/-}$ males present a reproductive abnormality characterized by a progressive loss of fertility that becomes evident at 5 months of age [16]. *mCd59ab*$^{-/-}$ males present a similar progressive loss of male fertility (Fig. 5a) with a lower efficiency in their ability to impregnate virgin wild type females (right panel in Fig. 5b). These reproductive abnormalities are not seen in littermate control *mCd59ab*$^{+/+}$ males. Analysis of sperm from 4-month-old *mCd59ab*$^{-/-}$ showed a significantly lower number of sperms when compared with *mCd59ab*$^{+/+}$ mice (Fig. 5c).

Discussion

Here, we describe (1) the successful generation of *mCd59a* and *mCd59b* double- knockout mice and (2) the phenotypic characterization of *mCd59ab*$^{-/-}$ mice in complement-sufficient (*C3*$^{+/+}$) and complement-deficient (*C3*$^{-/-}$) conditions with emphasis on the role of complement in the hemolytic anemia characteristically seen in Cd59 deficient mice.

FACS analysis with anti mCd59a and mCd59b specific antibodies has established the presence of both proteins in mouse red blood cells (mRBC) [20,21]; using the same antibodies, we now document the presence of mCd59a and mCd59b in mouse platelets. Similar to the observation in mRBC, the density of mCd59b in platelets is significant lower than that of mCd59a. Total abrogation of mCd59 function in *mCd59ab*$^{-/-}$ mice makes mRBC significantly more sensitive to complement mediated lysis induced through four different complement-activating assays (Fig. 3a–d). This increased sensitivity to complement-mediated lysis is not due to a concomitant down-regulation of *mDAF* or *mCrrY*, two additional complement-regulatory proteins in the mRBC membrane (Fig. 3f).

Consistent with an increased sensitivity to complement-mediated lysis of mRBCs *ex-vivo*, *mCd59ab*$^{-/-}$ mice exhibit the expected hemolytic anemia phenotype with (1) increased plasma-free hemoglobin clearly observed after inducing complement activation with CVF and (2) increased reticulocyte counts expressive of bone marrow stress.

We previously reported the generation of the *mCd59b*$^{-/-}$ mouse that exhibited a strong PNH-like phenotype in a B6/129 mixed genetic background [16]. Availability of anti-mCd59a monoclonal antibodies (kindly provided by Dr. B. P. Morgan) later revealed that *mCd59b*$^{-/-}$'s RBC also had a significant down-regulation of mCd59a. Together, the genetic background and the unintended downregulation of mCd59a explain the strong hemolytic phenotype of the *mCd59b*$^{-/-}$ mouse reported in [16]. In the *mCd59ab*$^{-/-}$ mouse reported here, we observe a 35% penetrance of the anemic phentoype, most likely explained by the different level of complement activity of individual mice in pure B6 background.

The finding of mCd59b expression in platelets confirms that this protein is expressed in other homeopathic cells, albeit at a lower level than mCd59a, similarly to mRBCs. The

collective experimental evidence obtained by us and others indicates that under physiological conditions, mCd59a is the primary source of CD59 anti-MAC activity in mice [20,21]. In the absence of mCd59a, protection of mRBC against MAC mediated hemolysis is conferred by mCd59b [20,21]. The generation of *mCd59ab*$^{-/-}$ mice devoted of any CD59 activity and their phenotyping under complement sufficient (*C3*$^{+/+}$) and complement deficient (*C3*$^{-/-}$) mice has helped confirm the critical role of CD59 in protecting RBC from complement (MAC)-mediated lysis.

The abnormal reproductive phenotype of *mCd59ab*$^{-/-}$ males is similar to that of *mCd59b*$^{-/-}$ mice [16]. The fact that *mCd59a*$^{-/-}$ does not show this peculiar loss of male fertility [15] together with the experiments with anti-mCd59a and mCd59b neutralizing antibodies reported in [22] indicate that the progressive loss of male fertility observed in *mCd59ab*$^{-/-}$ and *mCd59b*$^{-/-}$ is caused by the absence of mCd59b.

Materials and Methods

Animal studies have been reviewed and approved by the Harvard Medical School Institutional Animal Care and Use Committee (Animal Welfare Assurance no. A3431-01; International Animal Care and Use Committee approval date: Jan 10, 2005).

Generation of *mCd59ab* double-knockout mice

Both mouse *Cd59* genes have four exons; together they span 45.6 kb in the mouse genome: 19 kb *for mCd59a*, 15 kb for *mCd59b*, and ~11.6 kb of intervening sequence 14. A 3-kb DNA fragment downstream of exon 2 of *mCd59a* was amplified using a bacterial artificial chromosome (BAC) that covers the *mCd59* genes as a template and cloned into the right multiple cloning sites of NTKV-1908 vector (Strategene, La Jolla, CA). A 6.8-kb DNA fragment upstream of exon 4 of the *mCd59b* gene was isolated from the phage genomic clone that covers the *mCd59b* gene 14 and cloned into the left side of multiple cloning sites of NTKV-1908 vector. In the NYKV-1908 vector, these two fragments flanked the neomycin resistance gene, forming a 9.8-kb homologous sequence gene-targeting construct capable of replacing the *Neo* gene for an appropriate 24 kb genomic fragment. The deleted sequence contains exon 4 of *mCd59b* and exons 1 and 2 of *mCd59a* (Fig. 1a). To enable negative selection against random integration, the thymidine kinase gene from the herpes simplex virus was also included at the 5′ end of the construct.

Embryonic stem cells derived from 129/Sv mice were transfected, and G418- resistant clones were screened for homologous recombination by Southern blot analysis using the external left-arm probe shown in Fig. 1a, and by PCR with forward primer P4 from the *Neo* gene and reverse primer P5 from the external region at the 3′ end (Fig. 1a), respectively (data not shown). Two independent cell lines with targeted deletion of *mCd59a and mCd59b* (ES1 and ES2, Fig. 1b) were separately microinjected into C57BL/6 (B6) blastocysts, and generation of Agouti mice followed established procedures. *mCd59ab*$^{+/-}$ proposita were identified by Southern blot analysis and intercrossed to produce *mCd59ab*$^{-/-}$, *mCd59ab*$^{+/-}$, and *mCd59ab*$^{+/+}$ littermates. For genotyping by PCR, we used the primer pair P1 (5′ gagtgagtggaggaagagttatagg 3′) and P3 (5′ tgccctttgtttttagtggttatag 3′) to amplify the corresponding fragment in the wild-type chromosome and the primer pair P2 (5′

atcaattctctagagctcgctgatc 3′) and P3 to amplify the corresponding fragment in the targeted chromosome (Fig. 1a). Furthermore, we introduced *mCd59ab*$^{-/-}$ mutation, which was originally generated using 129/Sv stem cells, into a pure B6 genetic background through back-crossing with B6 mice eight times.

Generation of mCd59ab$^{-/-}$/C3$^{-/-}$ triple-knockout mice

To obtain *mCd59ab*$^{-/-}$/*C3*$^{-/-}$ mice, we crossed *mCd59ab*$^{-/-}$/*C3*$^{+/+}$ (in B6 background) with *mCd59ab*$^{+/+}$/*C3*$^{-/-}$ (in B6 background, purchased from Jackson Laboratory) to generate *mCd59ab*$^{+/-}$/*C3*$^{+/-}$. Intercrossing *mCd59ab*$^{+/-}$/*C3*$^{+/-}$ generated *mCd59ab*$^{-/-}$/*C3*$^{-/-}$ and *mCd59ab*$^{+/+}$/*C3*$^{+/+}$ offspring, which were identified by genotyping as described above (for *mCd59ab* deletion) and in [23] (for *C3* gene deletion).

Northern blot analysis

Total RNA from multiple tissues (fat tissue, testes, kidney, liver, lung, heart, and brain) of *mCd59ab*$^{-/-}$ and *mCd59ab*$^{+/+}$ was isolated using the *TRIZOL* reagent (Invitrogen, Carlsbad, CA) and hybridized with the ^{32}P-labeled *mCd59a*- or *mCd59b*-specific probe from *mCd59a* or *mCd59b* exon 4, as described [14].

Platelet preparation

Blood was collected by venipuncture from the mouse inferior vena cava into a syringe containing 500 μl Alsever's solution (72.4 mM NaCl, 31 mM sodium citrate, and 113.9 mM glucose) in the presence of 5 ng/ml PGI_2 (Cayman chemical, Ann Arbor, MI) to avoid aggregation, centrifuged (200*g* for 7 min at room temperature), and the supernatant [platelet-rich plasma (PRP)] spun down again (2,200*g* for 10 min at room temperature) to collect the platelet pellet. FACS analysis with anti-CD41 antibody was used to verify the purity of this platelet population (Fig. 2a).

FACS analysis

Platelets prepared as described above were fixed using 1% formaldehyde/PBS (2 hr at 4°C). Platelets were incubated with anti-mCd59a and anti-mCd59b (all kindly provided by Dr. B. P. Morgan), anti-mouse CD41 (Serotec, Raleigh, NC), anti-mouse DAF (kindly provided by Dr. E. Medof), or anti-mouse Crry (BD PharMingen San Diego, California 92121) (30 min at room temperature); washed, and incubated with a FITC-conjugated corresponding secondary antibody. The cells were washed in PBS three times before analyzing the fluorescence intensity using a FACScan (Becton Dickinson, Franklin Lakes, NJ).

Ex vivo complement-mediated assays on mouse erythrocytes

Sensitivity of mouse erythrocytes to either rat or mouse complement-mediated lysis was assessed by four different methods: (1) acidified serum lysis assay (Ham's test) [24]; (2) CVF lysis assay; (3) antibody-sensitized erythrocyte method; and (4) MAC-formation by C5b-7 site assay, all as described in Holt et al. [15]. In all cases, hemoglobin in the supernatant of lysed erythrocytes was measured by the absorbance at 414 nm, and percent lysis was calculated as: $\%\,\mathrm{LYSIS} = (\mathrm{test\ OD}_{414}^{-}\,\mathrm{blank\ OD}_{414}/\mathrm{total\ lysis\ OD}_{414}) \times 100$.

Reticulocyte count

The reticulocyte count of age-matched litter-mate—*mCd59ab*$^{-/-}$, *mCd59ab*$^{+/-}$, and *mCd59ab*$^{+/+}$ mice was analyzed by the method described in prior references [25,26]. Briefly, 5-μl tail vein blood collected in heparinized microcapillary tubes was stained with 50 μl 0.1% acridine orange in phosphate-buffered saline at room temperature for 30 min. Stained reticulocytes were counted under a fluorescent microscope using a Neubauer chamber.

Sperm count

A total of 10 ul of the sperm suspension diluted 1/10 into saline-buffered formaldehyde in a microcentrifuge tube was used to count sperm cells on a hemocytometer as described in Ref [21].

Assessment of the hematologic profile

250 μl aliquot of mouse blood will be analyzed on an Advia 120 auto-analyzer (Abbott, Chicago, IL), previously shown to generate reproducible blood cell parameters from mouse blood. Free hemoglobin in plasma will be determined by reading the OD_{414}.

Statistical analysis

The two groups were compared using 2-tailed Student *t* test for unpaired data. Data are presented as mean ± SEM. Level of significance for all comparisons was established at 0.05.

Acknowledgments

Contract grant sponsor: NIH; Contract grant numbers: RO1 DK060979, RO1052855, RO1 AI061174; Contract grant sponsor: American Heart Association; Contract grant number: 0435483N.

The authors are grateful to Dr. B. P. Morgan for providing anti-mCd59a and mCd59b monoclonal antibodies and Dr. E. Medof for providing anti-mDAF antibody.

References

1. Walport MJ. Complement. First of two parts. N Engl J Med. 2001; 344:1058–1066. [PubMed: 11287977]
2. Zhou X, Hu W, Qin X. The role of complement in the mechanism of action of rituximab for B-cell lymphoma: Implications for therapy. Oncologist. 2008; 13:954–966. [PubMed: 18779537]
3. Benzaquen LR, Nicholson-Weller A, Halperin JA. Terminal complement proteins C5b-9 release basic fibroblast growth factor and platelet-derived growth factor from endothelial cells. J Exp Med. 1994; 179:985–992. [PubMed: 8113689]
4. Halperin JA, Taratuska A, Nicholson-Weller A. Terminal complement complex C5b-9 stimulates mitogenesis in 3T3 cells. J Clinical Invest. 1993; 91:1974–1978. [PubMed: 8486768]
5. Acosta J, Qin X, Halperin J. Complement and complement regulatory proteins as potential molecular targets for vascular diseases. Curr Pharm Des. 2004; 10:203–211. [PubMed: 14754399]
6. Nicholson-Weller A, Halperin JA. Membrane signaling by complement C5b-9, the membrane attack complex. Immunol Res. 1993; 12:244–257. [PubMed: 8288945]
7. Morgan, BP.; Harris, CL. Complement Regulatory Proteins. London: Academic Press; 1999.
8. Walport MJ. Complement. Second of two parts. N Engl J Med. 2001; 344:1140–1144. [PubMed: 11297706]

9. Takeda J, Miyata T, Kawagoe K, et al. Deficiency of the GPI anchor caused by a somatic mutation of the PIG-A gene in paroxysmal nocturnal hemoglobinuria. Cell. 1993; 73:703–711. [PubMed: 8500164]
10. Hillmen P, Richards SJ. Implications of recent insights into the pathophysiology of paroxysmal nocturnal haemoglobinuria. Br J Haematol. 2000; 108:470–479. [PubMed: 10759701]
11. Luzzatto L, Bessler M. The dual pathogenesis of paroxysmal nocturnal hemoglobinuria. Curr Opin Hematol. 1996; 3:101–110. [PubMed: 9372059]
12. Parker CJ. Molecular basis of paroxysmal nocturnal hemoglobinuria. Stem Cells. 1996; 14:396–411. [PubMed: 8843541]
13. Qian YM, Qin X, Miwa T, et al. Identification and functional characterization of a new gene encoding the mouse terminal complement inhibitor CD59. J Immunol. 2000; 165:2528–2534. [PubMed: 10946279]
14. Qin X, Miwa T, Aktas H, et al. Genomic structure, functional comparison, and tissue distribution of mouse Cd59a and Cd59b. Mamm genome. 2001; 12:582–589. [PubMed: 11471050]
15. Holt DS, Botto M, Bygrave AE, et al. Targeted deletion of the CD59 gene causes spontaneous intravascular hemolysis and hemoglobinuria. Blood. 2001; 98:442–449. [PubMed: 11435315]
16. Qin X, Krumrei N, Grubissich L, et al. Deficiency of the mouse complement regulatory protein mCd59b results in spontaneous hemolytic anemia with platelet activation and progressive male infertility. Immunity. 2003; 18:217–227. [PubMed: 12594949]
17. Qin X, Ferris S, Hu W, et al. Analysis of the promoters and 5′-UTR of mouse Cd59 genes, and of their functional activity in erythrocytes. Genes Immun. 2006; 7:287–297. [PubMed: 16541098]
18. Acosta J, Hettinga J, Fluckiger R, et al. Molecular basis for a link between complement and the vascular complications of diabetes. Proc Natl Acad Sci USA. 2000; 97:5450–5455. [PubMed: 10805801]
19. Bodian DL, Davis SJ, Morgan BP, Rushmere NK. Mutational analysis of the active site and antibody epitopes of the complement-inhibitory glycoprotein, CD59. J Exp Med. 1997; 185:507–516. [PubMed: 9053451]
20. Baalasubramanian S, Harris CL, Donev RM, et al. CD59a is the primary regulator of membrane attack complex assembly in the mouse. J Immunol. 2004; 173:3684–3692. [PubMed: 15356114]
21. Qin X, Dobarro M, Bedford SJ, et al. Further characterization of reproductive abnormalities in mCd59b knockout mice: A potential new function of mCd59 in male reproduction. J Immunol. 2005; 175:6294–6302. [PubMed: 16272280]
22. Donev RM, Sivasankar B, Mizuno M, Morgan BP. The mouse complement regulator CD59b is significantly expressed only in testis and plays roles in sperm acrosome activation and motility. Mol Immunol. 2008; 45:534–542. [PubMed: 17597212]
23. Wessels MR, Butko P, Ma M, et al. Studies of group B streptococcal infection in mice deficient in complement component C3 or C4 demonstrate an essential role for complement in both innate and acquired immunity. Proc Natl Acad Sci USA. 1995; 92:11490–11494. [PubMed: 8524789]
24. Ham T. Chronic haemolytic anaemia with paroxysmal nocturnal haemoglobinuria: A study of the mechanism of haemolysis in relation to acid-base equilibrium. N Engl J Med. 1937; 217:915–917.
25. Thaer A, Becker H. Microscope fluorometric investigations on the reticulocytic maturation distribution as diagnostic criterion of disordered erythropoiesis. Blut. 1975; 30:339–348. [PubMed: 48388]
26. Abbrecht PH, Malvin RL, Vander AJ. Renal production of erythropoietin and renin after experimental kidney infarction. Nature. 1966; 211:1318–1319. [PubMed: 5969823]

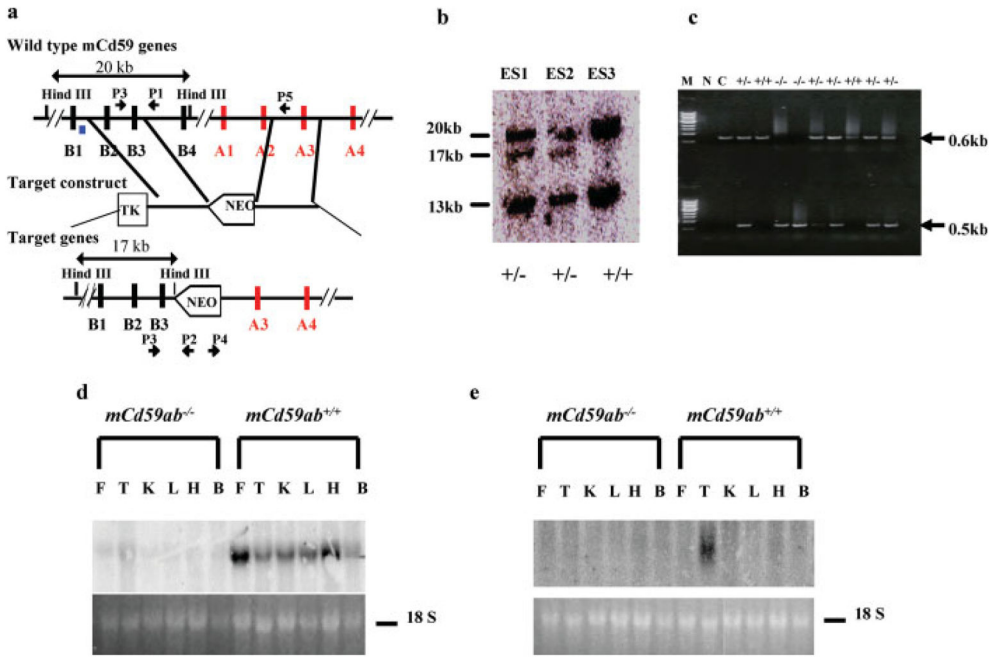

Figure 1.

Generation of *mCd59ab*$^{-/-}$ mice. (a) Target vector constructed to replace the genomic region spanning exon 4 of *mCd59b* and exon 1 and exon 2 of *mCd59a* by the *Neo* gene. Double-headed arrows indicate the size of the fragments seen in Southern blot analysis of wildtype (top) and targeted (bottom) alleles after the external probe (blue box) hybridized to Hind III digestion of genomic DNA. Black rectangles: *mCd59b* exons; red rectangles: *mCd59a* exons. (b) Southern analysis with external probe (blue square shown in Fig. 1a) to determine the homologous recombination of left arm. The 20, 17, and 13 kb Hind III bands represent expected wild-type, targeted fragment, and nonspecific binding fragment, respectively. (c) *mCd59ab*$^{-/-}$ genotyping by PCR. Top panel: PCR amplification of the wildtype fragment (expected 600 bp fragment with P1, a reverse primer matching the upstream region of deleted fragment; and P3, a forward primer matching the left arm shown in Fig. 1a). Bottom panel: PCR amplification of the target fragment (expected 500 bp fragment with P2, a reverse primer matching the upstream region of Neo; and P3, a forward primer matching the left arm shown in Fig. 1a). M: 1 kb ladder, N: negative control and C: positive 129 mouse strain control DNA for wildtype fragment. (d)–(e) Northern analysis of the *mCd59a* (d) or *mCd59b* (e) mRNA expression in multiple tissues of *mCd59ab*$^{+/+}$ and *mCd59ab*$^{-/-}$ mice. Top panel was blotted with *mCd59a* (d) or *mCd59b* (e) cDNA probe, and bottom panel is loading control. F, fat tissues; T, testes; K, kidney; L, liver; H, heart; B, brain.

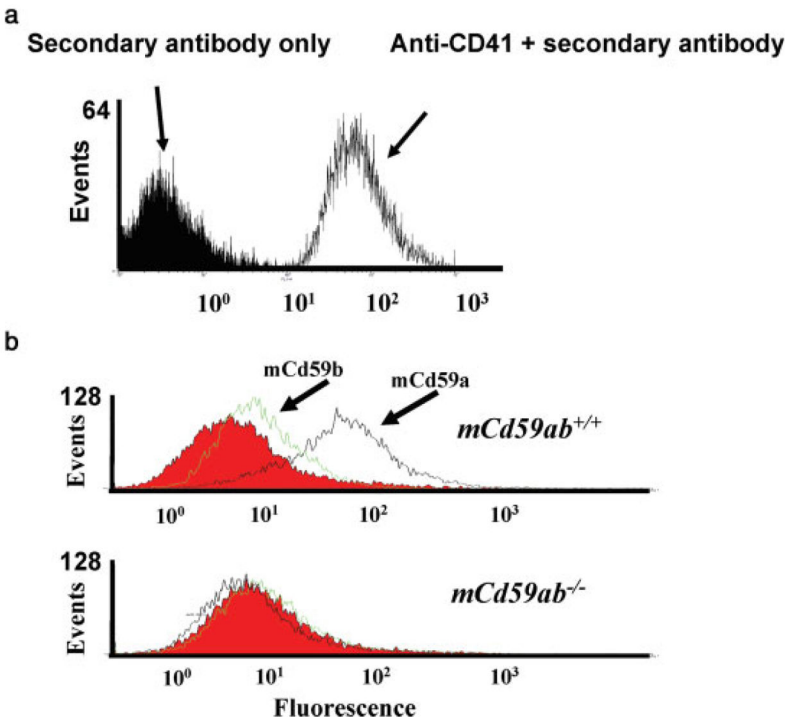

Figure 2.

The deficiency of mCd59a and mCd59b protein in the platelets of mCd59ab$^{-/-}$ mice. (a) The predominance of platelets in the cell population studied by FACS was confirmed with an antibody specific for the platelet marker CD41. (b) FACS analysis of the mCd59a or mCd59b proteins in platelets from *mCd59ab*$^{+/+}$ and *mCd59ab*$^{-/-}$ mice. Red area under the curve: FITC-secondary antibody only; Blue curve: mCd59b antibody plus FITC-secondary antibody, and Purple curve: mCd59a antibody plus FITC-secondary antibody.

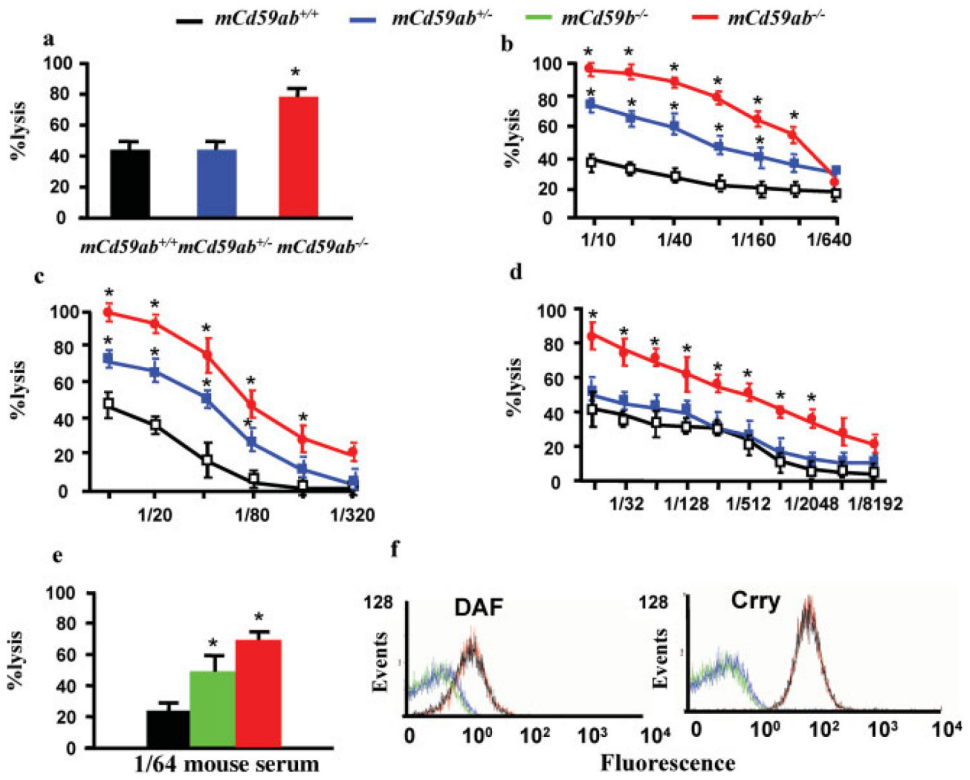

Figure 3.

mCd59ab$^{-/-}$ erythrocytes are more sensitive to complement-mediated lysis. (a) Ham's test (b) CVF-mediated erythrocytes lysis with rat serum. (c) Classical pathway assay in antibody-sensitized erythrocytes exposed to rat serum. (d) C5b-7 site assay. Erythrocytes bearing preformed C5b-7 sites were incubated with mouse serum. (e) Comparison of the sensitivity of *mCd59ab*$^{-/-}$ (red square) with *mCd59b*$^{-/-}$ erythrocytes (blue square) to complement-mediated lysis with C5b-7 site assay with mouse serum. Result are mean ± SEM off three mice per group. These experiments were repeated four times. *$P < 0.05$ vs. *mCd59ab*$^{+/+}$ mice. All other pair wise comparisons vs. *mCd59ab*$^{+/+}$ mice were not statistically significant. (f) FACS analysis of DAF and Crry expression in *mCd59ab*$^{-/-}$ and *mCd59ab*$^{+/+}$. Green curve: *mCd59ab*$^{+/+}$ erythrocytes stained with FITC-secondary antibody only, Blue curve: *mCd59ab*$^{-/-}$ erythrocytes stained with FITC-secondary antibody only, Black curve: *mCd59ab*$^{+/+}$ erythrocytes stained with primary plus FITC-secondary antibody and Red curve: *mCd59ab*$^{-/-}$ erythrocytes stained with primary plus FITC-secondary antibody.

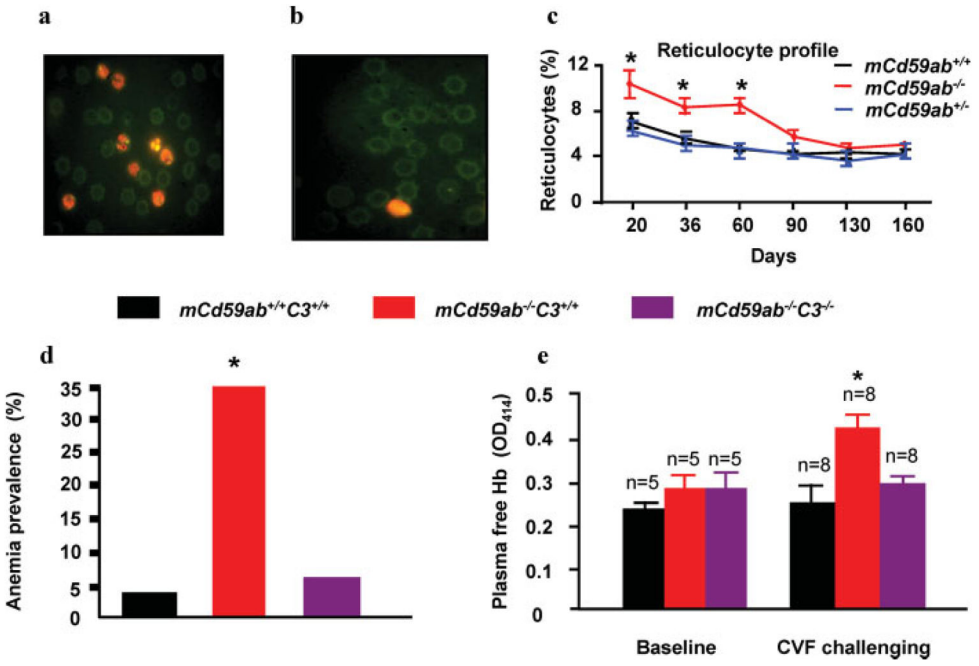

Figure 4.

Complement-mediated hemolytic anemia in *mCd59ab*$^{-/-}$. (a) and (b) Fluorescence staining of reticulocytes in blood smears from *mCd59ab*$^{-/-}$ (a) and *mCd59ab*$^{+/+}$(b). (c) Reticulocyte count profile in *mCd59ab*$^{+/+}$ and *mCd59ab*$^{-/-}$. *: *mCd59ab*$^{-/-}$/*C3*$^{+/+}$ vs. *mCd59ab*$^{+/+}$/*C3*$^{+/+}$ or *mCd59ab*$^{-/-}$/*C3*$^{-/-}$, $P < 0.01$, $n = 12$. (d) Percentage of anemic mice (Hb < 13g/dl at 2–4 month of age): *mCd59ab*$^{-/-}$/*C3*$^{+/+}$ ($n = 30$), *mCd59ab*$^{+/+}$/*C3*$^{+/+}$ ($n = 34$) and *mCd59ab*$^{-/-}$/*C3*$^{-/-}$ ($n = 14$). We compared the proportions in the extremes of the distributions using Fisher's exact test as described in21. *$P < 0.01$ vs. *mCd59ab*$^{+/+}$/*C3*$^{+/+}$. (e) C3 deficiency rescues the CVF induced intravascular hemolysis in *mCd59ab*$^{-/-}$. CVF (1 lg/gram body weight) (Complement Technology, Tyler, TX)15 was injected i.p. 24 hr before sacrifice by heart puncture. The level of free hemoglobin in a 1 to 10 dilution in PBS in plasma was determined by absorbance at 414 nm. *$P < 0.001$, vs. *mCd59ab*$^{+/+}$/*C3*$^{+/+}$ or *mCd59ab*$^{-/-}$/*C3*$^{-/-}$.

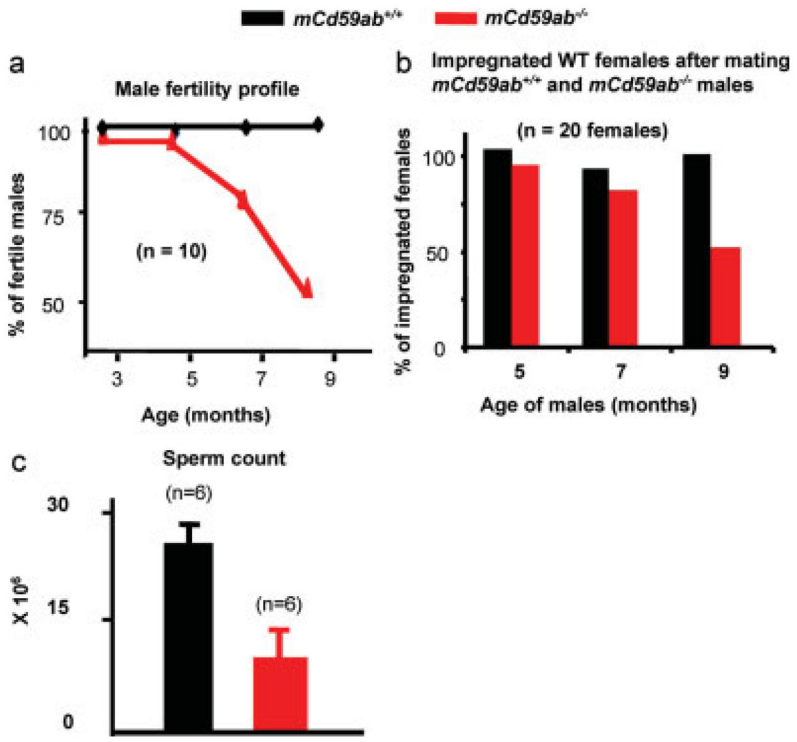

Figure 5.

Progressive loss of male fertility associated with lower sperm number in *mCd59ab*$^{-/-}$. (a) Male reproductive profile in *mCd59ab*$^{-/-}$ and *mCd59ab*$^{+/+}$. Infertility was defined by the failure to impregnate young *mCd59ab*$^{+/+}$ females after three consecutive matings: each males was mate with three different *mCd59ab*$^{+/+}$ females. (b) The percentage of impregnated normal females by *mCd59ab*$^{-/-}$ and *mCd59ab*$^{+/+}$ males of different ages. (c) Sperm count in *mCd59ab*$^{-/-}$ and *mCd59ab*$^{+/+}$ at the age of 4 months. *$P < 0.0001$ vs. *mCd59ab*$^{+/+}$.

TABLE I

Deficiency of mCd59a and mCd59b Protein in the Platelets of *mCd59ab*$^{-/-}$

Mouse proteins	Cd41 (FDU)	mCd59a (FDU)	mCd59b (FDU)
mCd59ab$^{+/+}$ (*n* = 4)	506.7 ± 44.2	10.4 ± 1.3*	1.6 ± 0.2*
mCd59ab$^{-/-}$ (*n* = 4)	589.7 ± 99.5	0.3 ± 0.5	0.18 ± 0.3

Actual fluorences density unit (FDU) equals FDU obtained by primary antibody and FITC-conjugated secondary antibody minus FDU obtained by FITC conjugated secondary antibody. Data are represented by Mean ± SEM.

* $P < 0.05$ vs. *mCd59ab*$^{-/-}$.

TABLE II

C3 Deficiency Rescues the Hemolytic Anemia in *mCd59ab*$^{-/-*}$

Mouse Genotype	Hemoglobin (Mean + SEM g/dl)
mCd59ab$^{+/+}$/*C3*$^{+/+}$ (*n* = 34)	14.7 ± 0.14
mCd59ab$^{+/-}$/*C3*$^{+/+}$ (*n* = 28)	14.7 ± 0.16[a]
mCd59ab$^{-/-}$/*C3*$^{+/+}$ (*n* = 30)	13.6 ± 1.0[b]
mCd59ab$^{-/-}$/*C3*$^{-/-}$ (*n* = 14)	14.2 ± 0.22[c]

*Mice are 2–4 months old.

[a]Comparison between *mCd59ab*$^{+/-}$/*C3*$^{+/+}$ and *mCd59ab*$^{+/+}$/*C3*$^{+/+}$, $P > 0.1$.

[b]Comparison between *mCd59ab*$^{-/-}$/*C3*$^{+/+}$ and *mCd59ab*$^{+/+}$/*C3*$^{+/+}$, $P < 0.01$.

[c]Comparison between *mCd59ab*$^{-/-}$/*C3*$^{-/-}$ and *mCd59ab*$^{+/+}$/*C3*$^{+/+}$, $P > 0.05$.